Identification and expression analysis of the zebrafish orthologues of mammalian *MAP1LC3* gene family

Swamynathan Ganesan [1*], Seyyed Hani Moussavi Nik[1], Morgan Newman[1], Michael Lardelli[1].

1. Discipline of Genetics, School of Molecular and Biomedical Sciences, The University of Adelaide, SA, 5005, Australia.

***Corresponding Author:**

Swamynathan Ganesan,

Zebrafish Genetics Laboratory,

School of Molecular and Biomedical Sciences,

The University of Adelaide, Adelaide SA 5005, Australia.

Tel. (+61) 88313 4863,

Fax (+61) 88313 4362.

Email: swamynathan.ganesan@adelaide.edu.au

Email Addresses of all authors:

Swamynathan Ganesan: swamynathan.ganesan@adelaide.edu.au

Seyyed Hani Moussavi Nik: seyyed.moussavinik@adelaide.edu.au

Morgan Newman: morgan.newman@adelaide.edu.au

Michael Lardelli: Michael.lardelli@adelaide.edu.au

Abstract

Autophagy is the principle pathway in a cell involved in clearing damaged proteins and organelles. Therefore autophagy is necessary to maintain turnover balance of peptides and homeostasis. Autophagy occurs at basal levels under normal conditions but can be upregulated by chemical inducers or stress conditions. The zebrafish (*Danio rerio*) serves as a versatile tool to understand the function of genes implicated in autophagy. We report the identification of the zebrafish orthologue of mammalian genes *MAP1LC3A (map1lc3a)* and *MAP1LC3B (map1lc3b)* by phylogenetic and conserved synteny analysis and examine their expression during embryonic development. Both the zebrafish *map1lc3a* and *map1lc3b* genes show maternally contributed expression in early embryogenesis. However, levels of *map1lc3a* transcript steadily increase until at least 120 hours post fertilisation (hpf) while the levels of *map1lc3b* show a more variable pattern across developmental time. We have also validated the LC3II/LC3I immunoblot assay in the presence of chloroquine (a lysosomal proteolysis inhibitor). We found that the LC3II/LC3I ratio is significantly increased in the presence of sodium azide treatment supporting that hypoxia induces autophagy in zebrafish. This was supported by our qPCR assay that showed an increase in *map1lc3a* transcript levels in the presence of sodium azide. In contrast levels of *map1lc3b* transcripts were reduced in the presence of rapamycin but showed no significant difference in the presence of sodium azide. Our study thus identifies the zebrafish orthologues of *MAP1LC3A & MAP1LC3B* and supports the use of zebrafish for the interaction between hypoxia, development and autophagy.

Keywords: Alzheimer's Disease, autophagy, LC3, hypoxia, rapamycin, chloroquine.

Introduction

The MAP (Microtubule associated protein) family encompasses a group of proteins that are found in association with microtubules [1]. MAP family proteins bind specifically to the microtubule lattice [2]. They are involved in microtubular assembly, organelle transport and cytoskeleton regulation [3]. They are abundantly expressed in the brain mainly during early developmental stages [4]. There are two peptide forms, namely MAP1A and MAP1B, which differ in their kinetic properties and phosphorylation mechanisms. They are highly expressed in neurons and are thought to play an important role in formation and development of neuronal cells [2]. Both these polypeptides consist of a heavy chain with different combinations of light chains [5]. One of the important light chains that is abundantly found in neurons is LC3 (light-chain 3) [5]. LC3 is proposed to be involved in the binding activities of MAP1A & MAP1B. Although both MAP1A & MAP1B are involved in stabilizing microtubules, they are also thought to play key roles in interacting with other signaling proteins involved in the MAP kinase pathway [2]. In most mammals, there are three different LC3 genes coding for three different polypeptides – *MAP1LC3A, MAP1LC3B* and *MAP1LC3C*. These peptides differ in their post-translational processing. *MAP1LC3A* and *MAP1LC3B* are well characterised and are thought to be involved in autophagy while the function of *MAP1LC3C* is not fully understood.

LC3 is a mammalian homologue of Atg8 (*Saccharomyces cerevisiae*) with 30% amino acid residue identity [6]. It is also one of the major biochemical markers of autophagy [7]. In the autophagy-lysosome pathway, long lived proteins and cellular components are degraded in the lysosome. This process is essential for normal cell homeostasis and for protein turnover [8]. Upon induction of autophagy LC3 binds with Phosphatidyl Ethanolamine (PE). This is essential for the extension and formation of autophagosomes [9]. It is also critical for cargo recognition in the lysosomes and for lysosomal degradation [10]. LC3 has two isoforms – LC3-I and LC3-II [11]. When autophagy is induced under normal conditions by starvation or by rapamycin treatment LC3-I is modified to LC3-II [12]. LC3-II is a secondary ubiquitinated form that binds with autophagosomes. After the autophagosome fuses with the lysosome, LC3-II is degraded by lysosomal proteases [11]. The rate of formation of LC3-II from LC3-I determines the autophagic flux and is used as a measure of autophagic activity.

The autophagic pathway occurs at basal levels under normal conditions but can be upregulated under stress conditions [13]. It plays a crucial role in various biochemical pathways of embryogenesis, growth, development and ageing [14]. Reports have suggested that autophagy can play a critical role in degrading neuritic amyloid peptides and neurofibrillary tangles which are pathological features observed in the progression of Alzheimer's disease (AD) [15]. Studies in AD patients have consistently shown failure of autophagy which clearly highlights the role played by this

process in AD [16]. Mutations in Amyloid-β A4 Precursor Protein (AβPP) and the PRESENILIN proteins (PSEN1 and PSEN2) which causes Familial Alzheimer's Disease (FAD) also play a key role in disrupting lysosomal function suggesting that these factors are linked. Studies have shown that Presenilins are required for lysosomal acidification and for the activation of lysosomal proteases during autophagy [17]. These studies suggest that autophagy may play a key role in AD progression.

In this paper, we identify the zebrafish orthologue of mammalian *MAP1LC3A* (*map1lc3a*) and *MAP1LC3B (map1lc3b)* by phylogenetic and conserved synteny analysis and examine their expression during embryonic development of zebrafish. Analysis of *map1lc3a* and *map1lc3b* function in zebrafish embryogenesis may be valuable for understanding their role in autophagy and the interplay of autophagy and other pathways in AD.

Materials and Methods

Ethics

This work was conducted under the auspices of The Animal Ethics Committee of The University of Adelaide and in accordance with EC Directive 86/609/EEC for animal experiments and the Uniform Requirements for Manuscripts Submitted to Biomedical Journals.

Zebrafish husbandry and experimental procedures

Danio rerio were bred and maintained at 28 °C on a 14 h light/10 h dark cycle. Embryos were collected from natural mating, grown in embryo medium (E3) and staged.

Phylogenetic and synteny analyses

The conserved regions of *map1lc3a and map1lc3b* protein sequences were aligned using Clustal W (Table 1) with a gap opening penalty of 10.0 and gap extension penalty of 3.0 for the pairwise alignment stage and a gap opening penalty of 10.0 and gap extension penalty of 5.0 for the multiple alignment stage [18]. Mr Bayes program was used for phylogenetic analysis [19]. The program was run under the JC69 (Juke–Cantor) model, with estimated proportion, estimated gamma distribution parameter, and optimized tree topology. Estimation of the tree reliability was carried out by the Maximum Likelihood Test Method [20] , using the GTR model as support.

For analysis of conservation of synteny for *map1lc3a*, the following loci were investigated: in humans, region 34.5–35.1 M of chromosome 20; in mouse, region 155.24–155.66 M of chromosome 2; in bovine, region 64.47–64.95 M of chromosome 13; and in zebrafish, region 26.11 – 27.55 of chromosome 11. The genes contained in the above regions were compared using the Sanger Ensembl (http://www.ensembl.org/Danio_rerio/Info/Index) and NCBI Entrez Gene databases (http://www.ncbi.nlm.nih.gov/gene) to identify homologues.

For analysis of conservation of synteny for *map1lc3b*, the following loci were investigated: in humans, region 87.3-87.9M of chromosome 16; in mouse, region 121.6-121.9M of chromosome 8; in bovine, region 13.0-13.4 M of chromosome 18; and in zebrafish, region 13.1-13.6M of chromosome 25. The genes contained in the above regions were compared using the Sanger Ensembl (http://www.ensembl.org/Danio_rerio/Info/Index) and NCBI Entrez Gene databases (http://www.ncbi.nlm.nih.gov/gene) to identify homologues.

RT-PCR assay and cloning of *map1lc3a* & *map1lc3b* cDNA

Total RNA was extracted from whole embryos at 2, 24, 48, 56, 72, 96, 120 h post-fertilization (hpf) using the QIAGEN RNeasy mini kit (QIAGEN, GmbH, Hilden, Germany). Zebrafish cDNAs were generated using 5 μg of total RNA from embryos by reverse transcription (Super script III kit; Invitrogen, Camarillo, USA). For PCR amplification, 5 μL of the cDNA was used with the primers: *map1lc3a F* (5′-CGAGTCGACCGACAATTTAGC-3′) and *map1lc3a R* (5′-TCCTTGCAACGATCAGCGAA-3′); *map1lc3b F* (5′- AATGTGACGATTGGACACGAGT -3′) and *map1lc3b R* (5′- AGTACAACAGCTCACGGTTATGC - 3′). Control PCR primers for zebrafish *β-actin* were: *β-actin F* (5′-TTCTGGTCGGTACTGGTATTGTG -3′) and *β-actin R* (5′- ATCTTCATCAGGTAGTCTGTCAGGTT -3′) [21].

PCR was performed using Dynazyme DNA polymerase (Finnzymes Oy, Espoo, Finland) for 35 cycles with a denaturation temperature of 94 °C for 30s, an annealing temperature of 60 °C for 30 s and an extension temperature of 72 °C for 2 min. The PCR products were cloned into the pGEM-T vector (Promega, Madison, USA) and sequenced.

Quantitative PCR

Quantitative real time PCR was performed using POWER SYBR Green PCR Master Mix (Applied Biosystems, Foster City, CA, USA) and the ABI 7000 Sequence Detection System (Applied Biosystems). The relative standard curve method for quantification was used to determine the expression of experimental samples compared to a basis sample. Gene specific primers were designed for amplification of *map1lc3a* (*Qmap1lc3a.F*: 5′-CGAGTCGACCGACAATTTAGC-3′ and *Qmap1lc3aR*: 5′-TCCTTGCAACGATCAGCGAA-3′), *map1lc3b* (*Qmap1lc3bF:5'*- AATGTGACGATTGGACACGAGT – 3' and *Qmap1lc3bR:* 5' – AGTACAACAGCTCACGGTTATGC – 3') and for the ubiquitously expressed control genes *eef1a1a* (*Qeef1a1aF:* 5′-CCAACTTCAACGCTCAGGTCA-3′ and *Qeef1a1aR:* 5′-CAAACTTGCAGGCGATGTGA-3′) and β-actin (*Q β-actinF*: 5′- TTCTGGTCGGTACTGGTATTGTG -3′and *β-actinR* : 5′- ATCTTCATCAGGTAGTCTGTCAGGTT -3′) [21].

cDNA was serially diluted (100 ng, 50 ng, 25 ng, and 12.5 ng per reaction) to generate the standard curve. Amplification conditions were 2 min at 50 °C followed by 10 min at 95 °C and then 40–45 cycles of 15 s at 95 °C and 1 min at 60 °C. The expression of *map1lc3a* in wild-type embryos at 2, 24, 48, 56, 72, 96, 120 hpf was analysed. All qPCRs were done in triplicate and three biological replicates were performed for each gene expression analysis. Cycle

thresholds obtained from each triplicate were averaged and normalized against the expression of *ef1a*. The fold changes of expression were determined by comparing each experimental sample to the basis sample.

Whole-mount in situ transcript hybridization (WISH)

Wild-type embryos were collected and dechorionated at 18, 24, 36, 48, 72, 96, 120 hpf for WISH. The embryos were then fixed in 4% formaldehyde in PBS at 4ºC overnight and stored in 100% methanol at -20ºC. A Digoxigenin-11-uridine-5′-triphosphate (DIG) antisense labeled RNA probe was then generated using SP6 or T7 RNA polymerase from a cDNA amplified from a clone using M13 primers. WISH was then performed as previously described [22].

Drug Treatment – Autophagy Inducers

Wild-type embryos were collected and treated with the following drugs dissolved in DMSO. Rapamycin, which is a known inducer of autophagy, was added to a final concentration of 1μM to 48hpf embryos for 24h [23, 24]. Chloroquine, a chemical that increases the lysosomal pH thus inhibiting autophagy was added at a concentration of 50μM to 56hpf embryos for 16h [25, 26]. Sodium Azide was used at a concentration of 100μM on 66hpf embryos for 6h. All embryos (wild-type & drug treated) were subjected to yolk-removal and lysis at 72hpf for immunoblotting.

Western immunoblot analyses

Dechorionated and deyolked embryos were placed in sample buffer (2% sodium dodecyl sulfate (SDS), 5% β-mercaptoethanol, 25% v/v glycerol, 0.0625 M Tris–HCl (pH 6.8), and bromphenol blue), heated immediately at 100◦C for 5 min, and then stored at –20◦C prior to protein separation on 15% SDS–polyacrylamide gels. Proteins were transferred to PVDF membranes using a semidry electrotransfer system. When immunoblotting with anti-LC3 antibodies, the membranes were blocked with 5% Western Blot Blocking Solution in TBST, incubated with a 1/2,000 dilution of primary antibodies in TBST containing 1% Western Blot Blocking Solution , washed in TBST, and incubated with a 1/10,000 dilution of anti-rabbit (Rockland Immunochemicals Inc., Gilbertsville, PA, USA). For incubation with anti-β-tubulin antibodies (Antibody E7, Developmental Studies Hybridoma Bank, The University of Iowa, IA, USA), the conditions were the same as for western immunoblotting with anti-LC3 antibodies except that the primary antibodies were diluted 1/200 and donkey antimouse IgG secondary antibodies (Jackson ImmunoResearch Laboratories Inc., West Grove, PA, USA) were diluted 1/10,000. After incubation with secondary antibodies, all the membranes were washed four times for 15 min in TBST and visualized with luminol reagents (Amresco, Ohio, USA) by exposure to X-ray films (GE Healthcare LTD, Amersham Hyperfilm ^{TM} ECL, UK) and the ChemiDoc™ MP imaging system (Bio-Rad, Hercules, CA, USA).

Statistical Analysis

Means and standard deviations were calculated for all variables using conventional methods. A Students t-test was used to evaluate significant differences among the groups. Each experiment was performed with 3 biological replicates. A criterion alpha level of $P<0.05$ was used for all statistical comparisons. All the data were analysed using GraphPad Prism version 6.0 (GraphPad Prism, La Jolla, CA).

Results

Identification of the zebrafish *map1lc3a* & *map1lc3b* gene by a phylogenetic approach

The *MAP1LC3A* and *MAP1LC3B* genes belong to the family of Microtubule Associated Proteins (MAP) [1]. These genes have been identified in major mammals (e.g., human, mouse, and bovine). To identify genes in zebrafish with possible orthology to *MAP1LC3A* and *MAP1LC3B*, we searched the NCBI and Ensembl genome databases using the human MAP1LC3A and MAP1LC3B protein sequences as probes.

A tBLASTn search of the NCBI database using MAP1LC3A as a probe identified a gene located on chromosome 11 (NM_214739.1) with high sequence homology. The E-value of tBLASTn alignments between human MAP1LC3A and this candidate was $3e^{-76}$ and was significantly smaller than other aligned sequences (E-value for next candidate was $2e^{-68}$). The amino acid (aa) residue identity between human MAP1LC3A and the putative protein sequence of the zebrafish candidate orthologue following Clustal W alignment (see Materials and Methods) is 96% (Figure 1A).

Similarly a tBLASTn search of the NCBI database using MAP1LC3B as a probe identified a gene located on chromosome 25 (NM_199604.1) with high sequence homology. The E-value of tBLASTn alignments between human MAP1LC3B and this candidate was $6e^{-74}$ and was significantly smaller than other aligned sequences (E-value for next candidate was $2e^{-65}$). The amino acid (aa) residue identity between human MAP1LC3B and the putative protein sequence of the zebrafish candidate orthologue following Clustal W alignment (see Materials and Methods) is 93% (Figure 1A).

Phylogenetic analysis was carried out using Mr.Bayes comparing the zebrafish genes with the DNA sequences of the *MAP1LC3A* orthologues of human, mouse, and bovine, as well as the most closely related MAP gene family members from all these species, i.e., *MAP1LC3B* and *MAP1LC3C* to examine the relationship between the zebrafish genes and other members of the *MAP1LC3* family. The results strongly support that the gene identified as *map1lc3a* and *map1lc3b*are zebrafish orthologues of human *MAP1LC3A* and *MAP1LC3B* respectively (Figure 1B).

Synteny conservation analysis supports the results of the phylogenetic analysis

Synteny conservation analysis was performed to confirm the results of the phylogenetic analysis. Neighbouring genes on each side of the zebrafish candidate genes were investigated using the Sanger Ensembl database. This led to the identification of three zebrafish genes, *trpc4apa, myh7ba, dynlRb1* that are apparent orthologues of genes syntenic with human *MAP1LC3A* on chromosome 11. Interestingly, while the relative orientations of the *map1lc3a* and *dynlrb1* genes are conserved between zebrafish and the mammals, a chromosomal rearrangement means that the

orientation of these two genes with respect to *trpc4apa* and *myh7ba* differs in zebrafish (Figure 2). For zebrafish *map1lc3b,* two genes, *zcchc1* and s*lc7a5 (LOC797250)* were identified that are orthologues of genes syntenic with human *MAP1LC3B* on chromosome 16 (Figure 3). The locations of orthologues of these syntenic genes in mouse and bovine were also identified. tBLASTn searches confirmed that these neighbouring genes of human *MAP1LC3A* and *MAP1LC3B* showed their highest levels of identity with their zebrafish counterparts indicated above rather than other homologues in the zebrafish genome thus supporting their identification as orthologues. Therefore, analysis of synteny conservation supports the proposed orthology between zebrafish *map1lc3a* and human *MAP1LC3A* and between zebrafish *map1lc3b* and human *MAP1LC3B.*

Embryonic and early larval expression of *map1lc3a & map1lc3b*

The temporal expression of *map1lc3a & map1lc3b* mRNA in zebrafish embryos and early larvae at different timepoints was examined using a RT-PCR assay. Zebrafish *map1lc3a* and *map1lc3b* were barely detectable in maternally contributed transcripts (i.e., at 2hpf) and were observed at relatively low levels by 24hpf. They were easily detectable by the end of embryogenesis (hatching) at 48hpf. Expression then continued through to adulthood. These observations were confirmed by quantitative RT-PCR (qRT-PCR) showing that the relative gene expression levels of *map1lc3a* and *map1lc3b* are much lower in embryos at early stages of development in comparison to in larvae at 96hpf & 120hpf (Figure 4). The expression of map1lc3a shows a fairly linear pattern of increase from 24hpf to 120hpf, relative to the *β-actin* standard used. In contrast, transcript levels of *map1lc3b* gene rose to an early peak at around 56hpf before declining until around 96hpf and then rising again by 120hpf (Figure 5A).

Whole Mount In-situ Transcript Hybridisation

To validate further the expression of *map1lc3a & map1lc3b* in zebrafish embryos, whole mount *in situ* hybridization was performed on zebrafish embryos. After extended staining (3 days at room temperature) no specific staining was observable for either gene at 48hpf indicating that the level of expression was too low to be detected by this technique. (As a positive control, the expected pattern of expression was observed in control embryos stained to reveal expression of neurogenin1 – data not shown).

Expression of zebrafish *map1lc3a* and *map1lc3b* following treatments to induce autophagy

To examine whether conditions known to induce autophagy cause increased transcript levels from the *map1lc3a* and *map1lc3b* genes, we examined their expression by qRT-PCR at 72hpf. Embryos at 48hpf were treated for a further 24h with rapamycin while another cohort of embryos was subjected to mimicry of hypoxia by exposure to sodium

azide for 6h starting at 66hpf (see Materials and Methods). Levels of *map1lc3a* and *map1lc3b* transcripts in these embryos were compared to control (untreated embryos at 72hpf). The qRT-PCR analysis showed that the relative levels of *map1lc3a* transcripts increase by approximately 1.4 fold under exposure to either rapamycin or sodium azide. In contrast levels of *map1lc3b* transcripts were reduced in the presence of rapamycin but showed no significant decrease in the presence of sodium azide. (Figure 5B).

Increased LC3II/LC3I ratio in the presence of lysosomal inhibitors indicates increased autophagy in zebrafish embryos

The initiation of autophagy in a cell can be detected by analysis of the conversion of LC3I to LC3II. Therefore an increase in the LC3II/LC3I ratio may indicate increased autophagic flux in cells. However, an increased LC3II/LC3I ratio alone is not accepted as sufficient to indicate increased autophagic flux [26]. For that, the LC3II/LC3I ratio must be shown to increase when lysosomal function is blocked, e.g. by chloroquine that increases lysosomal pH [26].

The mammalian *MAP1LC3A* and *MAP1LC3B* genes encode very similar proteins and the zebrafish orthologues of these genes are expected to do the same. Antibodies against "LC3" detect both proteins and are used in western immunoblot assays to monitor autophagy activity. He et al used an antibody against mammalian LC3 to monitor the LC3II/LC3I ratio in zebrafish but this approach has not yet been validated in zebrafish using the lysosomal inhibitor chloroquine [24]. Therefore, we used the same antibody to examine the LC3II/LC3I ratio in zebrafish embryos at 72hpf with and without chloroquine and in the presence or absence of autophagy inducers rapamycin and sodium azide. In every case, including otherwise untreated control embryos, we observed a significant increase in the LC3II/LC3I ratio in the presence of chloroquine indicating the increased autophagic flux (Figure 6). This experiment also confirmed the ability of rapamycin and chemical mimicry of hypoxia (sodium azide treatment) to increase the rate of autophagy in zebrafish (Figure 6).

Discussion

Autophagy is the principle pathway in cells involved in clearing damaged proteins and organelles. It is, therefore critical to cell survival [27]. Autophagy has been widely studied in relation to various diseases including AD. Failure in autophagy due to mutations in the *PRESENILIN 1* gene has been implicated in AD [28]. To gain greater insight into autophagy, various animal models have been used to study the components of the autophagic pathway. However, only limited analysis has been performed using zebrafish (see below) despite its utility as a model organism in AD research [29].

A number of studies have described assays for autophagy in zebrafish. A transgenic zebrafish line bearing a fusion of GFP to MAP1LC3B has been constructed and used for monitoring of autophagy [24]. Also, immunoblot assays using antibodies against LC3 are commonly used to monitor induction of autophagy [30-34]. However, the zebrafish orthologues of the *MAPLC3A* and *MAP1LC3B* genes that code for LC3 remain poorly characterised. The primary aim of this study was to identify zebrafish orthologues of these genes for analysis of their expression in embryos and early larvae. Using phylogenetic and synteny conservation analysis we confirmed the presence of the orthologous genes in zebrafish, *map1lc3a* & *map1lc3b*

Both the zebrafish *map1lc3a* and *map1lc3b* genes show maternally contributed expression in early embryogenesis. However, levels of *map1lc3a* transcript steadily increase until at least 120hpf while the levels of *map1lc3b* show a more variable pattern across developmental time. The reason for this is unknown but the retention of these two genes that encode very similar proteins over more than 450 million years since the divergence of teleosts and tetrapods indicates that they probably have very important unique functions in autophagy and protein turnover in addition to any functional redundancy. This idea is supported by the increased levels of *map1lc3a* transcripts seen when autophagy is induced by rapamycin and mimicry of hypoxia while *map1lc3b* transcript levels decreased under treatment with rapamycin and showed no significant change under mimicry of hypoxia.

In mammalian systems, increased levels of LC3II or increase in the LC3II/LC3I ratio suggest either an induction of autophagosome formation and autophagic flux or a failure in autophagosome turnover [24]. To differentiate between these two possibilities it is now *de rigeur* to carry out western immunoblotting against LC3I and LC3II in the presence of lysosomal inhibitors. An increase in LC3II/LC3I ratio in the presence of a lysosomal inhibitor supports that there is an induction in the formation of autophagosomes and increased autophagic flux [26]. We have used chloroquine to demonstrate that the LC3II/LC3I ratio is significantly increased by exposure of zebrafish larvae to rapamycin or sodium azide (for mimicry of hypoxia) in their aqueous medium.

Our study supports that it is possible to analyse autophagy *in vivo* using zebrafish embryos/larvae. This is important since mammalian cells grown in culture are under stress, and show unusual patterns of gene expression due to absence of their unusual growth medium and have an absence of their normal three-dimensional cellular contacts. Furthermore, immortalised cells have altered gene expression patterns. Nevertheless, the effects of various chemicals on autophagy can be analysed simply by their placement in the water/aqueous medium in which zebrafish embryos/larvae grow and develop. The ability to analyse autophagy in zebrafish embryos/larvae enhances the use of the zebrafish for investigation of the molecular mechanisms underlying Alzheimer's disease.

Figure Captions

Table 1 – Protein sequences used in the phylogenetic analysis

Figure 1 – (A) Alignment of the putative amino acid residue sequences of the zebrafish *map1lc3a* and *map1lc3b* candidates with the MAP1LC3A and MAP1LC3B proteins of humans, the mouse and bovines. The alignment was performed using Clustal W with gap opening penalty of 10.0 and gap extension penalty of 3.0 for the pairwise alignment stage and a gap opening penalty of 10.0 and gap extension penalty of 5.0 for the multiple alignment stage. Black shading indicates the identical residues. (B) Phylogenetic tree of the MAP1LC3A and MAP1LC3B protein family generated using MrBayes. Numbers represent the aLRT branch – support values. Sequences used in the phylogenetic analysis are shown in Table 1.

Table 2 – Summary of tBLASTn search results in the analysis of synteny conservation for *map1lc3a*. Highest quality hits are shown in descending order. Probes were translations of full-length open reading frames of the relevant genes.

Figure 2 – Schematic showing genes syntenic with the proposed zebrafish orthologue of human *MAP1LC3A* and those syntenic with the human (Hs), mouse (Mm) and bovine (Bt) *MAP1LC3A* genes. The chromosomal positions of these genes are shown on the numbered baselines. Numbers on the baselines indicate gene positions on the chromosomes (M= megabases) (http://www.ensembl.org/Danio_rerio/Info/Index). Arrows indicate the direction of gene transcription. The table shows the orthology relationships between genes in different organisms.

Table 3 – Summary of tBLASTn search results in the analysis of synteny conservation for *map1lc3b*. Highest quality hits are shown in descending order. Probes were translations of full-length open reading frames of the relevant genes.

Figure 3 – Schematic showing genes syntenic with the proposed zebrafish orthologue of human *MAP1LC3B* and those syntenic with the human (Hs), mouse (Mm) and bovine (Bt) *MAP1LC3B* genes. The chromosomal positions of these genes are shown on the numbered baselines. Numbers on the baselines indicate gene positions on the chromosomes (M= megabases) (http://www.ensembl.org/Danio_rerio/Info/Index). Arrows indicate the direction of gene transcription. The table shows the orthology relationships between genes in different organisms.

Figure 4- RT-PCRs detecting *map1lc3a* & *map1lc3b* transcripts at different developmental stages.

Figure 5 – (A) Relative gene expression level profiles of *map1lc3a* and *map1lc3b* mRNA at different developmental stages determined by qRT-PCR. The expression levels of *map1lc3a* and *map1lc3b* between samples were normalized

against *β-actin.* Each experiment was replicated completely three times with triplicate PCRs performed for each replicate. Error bars show standard deviation (S.D).

(B) Relative gene expression level profile of *map1lc3a* and *map1lc3b* mRNA at 72h including after exposure to rapamycin and to sodium azide (to mimic hypoxia). The expression levels of *map1lc3a* and *map1lc3b* are normalized against *eef1a1a.* Each experiment was replicated three times and triplicate PCRs were performed for each replicate. Error bars show standard errors of the means.

Figure 6 – (A) Use of chloroquine in LC3II/I assays of autophagy in zebrafish larvae. Treatment of embryos with rapamycin or sodium azide was performed as described above. Embryos were deyolked at 72h, lysed and subjected to SDS-PAGE before LC3II and LC3I were detected using anti-LC3 antibody. Anti-tubulin antibody was used as a loading control. (B) The LC3II/LC3I ratio was calculated using Image Lab software. The ratio for the control samples was adjusted to 1.0 and the other ratios were normalised to this. Each analysis was carried out in triplicate. Error bars show standard errors of the means.

Con – Control, Rap - Rapamycin, Chl – Chloroquine, S/A - Sodium Azide.

Acknowledgements

This research was supported by funds from the School of Molecular and Biomedical Science and by an Adelaide Scholarship International to SG from the University of Adelaide. MN is supported by funds from the Australian National Health and Medical Research Council (APP1061006). The sources of funding listed above played no role in the study design; in the collection, analysis and interpretation of data; in the writing of the report; or in the decision to submit the paper for publication. The authors declare that they have no conflict of interest in this work.

References

1. Vallee, R.B., G.S. Bloom, and W.E. Theurkauf, *Microtubule-associated proteins: subunits of the cytomatrix.* The Journal of cell biology, 1984. **99**(1 Pt 2): p. 38s-44s.
2. Halpain, S. and L. Dehmelt, *The MAP1 family of microtubule-associated proteins.* Genome biology, 2006. **7**(6): p. 224.
3. Schoenfeld, T.A., et al., *MAP 1A and MAP 1B are structurally related microtubule associated proteins with distinct developmental patterns in the CNS.* The Journal of neuroscience : the official journal of the Society for Neuroscience, 1989. **9**(5): p. 1712-30.
4. Bloom, G.S., F.C. Luca, and R.B. Vallee, *Identification of high molecular weight microtubule-associated proteins in anterior pituitary tissue and cells using taxol-dependent purification combined with microtubule-associated protein specific antibodies.* Biochemistry, 1985. **24**(15): p. 4185-91.
5. Mann, S.S. and J.A. Hammarback, *Molecular characterization of light chain 3. A microtubule binding subunit of MAP1A and MAP1B.* The Journal of biological chemistry, 1994. **269**(15): p. 11492-7.
6. Tanida, I., T. Ueno, and E. Kominami, *LC3 and Autophagy.* Methods in molecular biology, 2008. **445**: p. 77-88.
7. Behrends, C., et al., *Network organization of the human autophagy system.* Nature, 2010. **466**(7302): p. 68-76.
8. Lingwood, D., et al., *Morphological homeostasis by autophagy.* Autophagy, 2009. **5**(7): p. 1039-40.
9. He, C. and D.J. Klionsky, *Regulation mechanisms and signaling pathways of autophagy.* Annu Rev Genet, 2009. **43**: p. 67-93.
10. Pankiv, S., et al., *p62/SQSTM1 binds directly to Atg8/LC3 to facilitate degradation of ubiquitinated protein aggregates by autophagy.* The Journal of biological chemistry, 2007. **282**(33): p. 24131-45.
11. Kabeya, Y., et al., *LC3, a mammalian homologue of yeast Apg8p, is localized in autophagosome membranes after processing.* The EMBO journal, 2000. **19**(21): p. 5720-8.
12. Tanida, I., T. Ueno, and E. Kominami, *LC3 conjugation system in mammalian autophagy.* Int J Biochem Cell Biol, 2004. **36**(12): p. 2503-18.
13. Kim, K.W., et al., *Autophagy upregulation by inhibitors of caspase-3 and mTOR enhances radiotherapy in a mouse model of lung cancer.* Autophagy, 2008. **4**(5): p. 659-68.
14. Mortimore, G.E., et al., *Autophagy.* Sub-cellular biochemistry, 1996. **27**: p. 93-135.
15. Yang, D.S., et al., *Therapeutic effects of remediating autophagy failure in a mouse model of Alzheimer disease by enhancing lysosomal proteolysis.* Autophagy, 2011. **7**(7): p. 788-9.
16. Nixon, R.A. and D.S. Yang, *Autophagy failure in Alzheimer's disease-locating the primary defect.* Neurobiol Dis, 2011. **43**(1): p. 38-45.
17. Lee, J.H., et al., *Lysosomal proteolysis and autophagy require presenilin 1 and are disrupted by Alzheimer-related PS1 mutations.* Cell, 2010. **141**(7): p. 1146-58.
18. Corpet, F., *Multiple sequence alignment with hierarchical clustering.* Nucleic Acids Res., 1988. **16**(22).
19. Huelsenbeck JP, R.F., *MRBAYES: Bayesian inference of phylogenetic trees.* Bioinformatics, 2001. **17**(8): p. 754-755.
20. Guindon S, G.O., *A simple, fast, and accurate algorithm to estimate large phylogenies by maximum likelihood.* Systems Biology. , 2003. **52**(5): p. 696-704.
21. Moussavi Nik, S.H., et al., *The BACE1-PSEN-AbetaPP regulatory axis has an ancient role in response to low oxygen/oxidative stress.* J Alzheimers Dis, 2012. **28**(3): p. 515-30.
22. Newman, M., et al., *Altering presenilin gene activity in zebrafish embryos causes changes in expression of genes with potential involvement in Alzheimer's disease pathogenesis.* J Alzheimers Dis, 2009. **16**(1): p. 133-47.
23. He, C. and D.J. Klionsky, *Analyzing autophagy in zebrafish.* Autophagy, 2010. **6**(5).
24. He, C., et al., *Assaying autophagic activity in transgenic GFP-Lc3 and GFP-Gabarap zebrafish embryos.* Autophagy, 2009. **5**(4): p. 520-6.
25. Cui, J., et al., *Generation of transgenic zebrafish with liver-specific expression of EGFP-Lc3: a new in vivo model for investigation of liver autophagy.* Biochem Biophys Res Commun, 2012. **422**(2): p. 268-73.
26. Klionsky, D.J., et al., *Guidelines for the use and interpretation of assays for monitoring autophagy.* Autophagy, 2012. **8**(4): p. 445-544.
27. Mizushima, N., *Autophagy: process and function.* Genes Dev, 2007. **21**(22): p. 2861-73.
28. Wolfe, D.M., et al., *Autophagy failure in Alzheimer's disease and the role of defective lysosomal acidification.* Eur J Neurosci, 2013. **37**(12): p. 1949-61.
29. Newman, M., et al., *Zebrafish as a tool in Alzheimer's disease research.* Biochim Biophys Acta, 2011. **1812**(3): p. 346-52.

30. Kim, S.H., et al., *Molecular cloning and expression analyses of porcine MAP1LC3A in the granulosa cells of normal and miniature pig.* Reprod Biol Endocrinol, 2013. **11**: p. 8.
31. Xiao, J., et al., *MiR-204 regulates cardiomyocyte autophagy induced by ischemia-reperfusion through LC3-II.* J Biomed Sci, 2011. **18**: p. 35.
32. Xie, B., et al., *Restoration of klotho gene expression induces apoptosis and autophagy in gastric cancer cells: tumor suppressive role of klotho in gastric cancer.* Cancer Cell Int, 2013. **13**(1): p. 18.
33. Bellot, G., et al., *Hypoxia-induced autophagy is mediated through hypoxia-inducible factor induction of BNIP3 and BNIP3L via their BH3 domains.* Mol Cell Biol, 2009. **29**(10): p. 2570-81.
34. Farg, M.A., et al., *C9ORF72, implicated in amytrophic lateral sclerosis and frontotemporal dementia, regulates endosomal trafficking.* Hum Mol Genet, 2014.

Figures

Figure 1 – (A) Alignment of the putative amino acid residue sequences of the zebrafish map1lc3a and map1lc3b candidates with the MAP1LC3A and MAP1LC3B proteins of humans, the mouse and bovines. The alignment was performed using Clustal W with gap opening penalty of 10.0 and gap extension penalty of 3.0 for the pairwise alignment stage and a gap opening penalty of 10.0 and gap extension penalty of 5.0 for the multiple alignment stage. Black shading indicates the identical residues. (B) Phylogenetic tree of the MAP1LC3A and MAP1LC3B protein family generated using MrBayes. Numbers represent the aLRT branch – support values. Sequences used in the phylogenetic analysis are shown in Table 1.

(A)

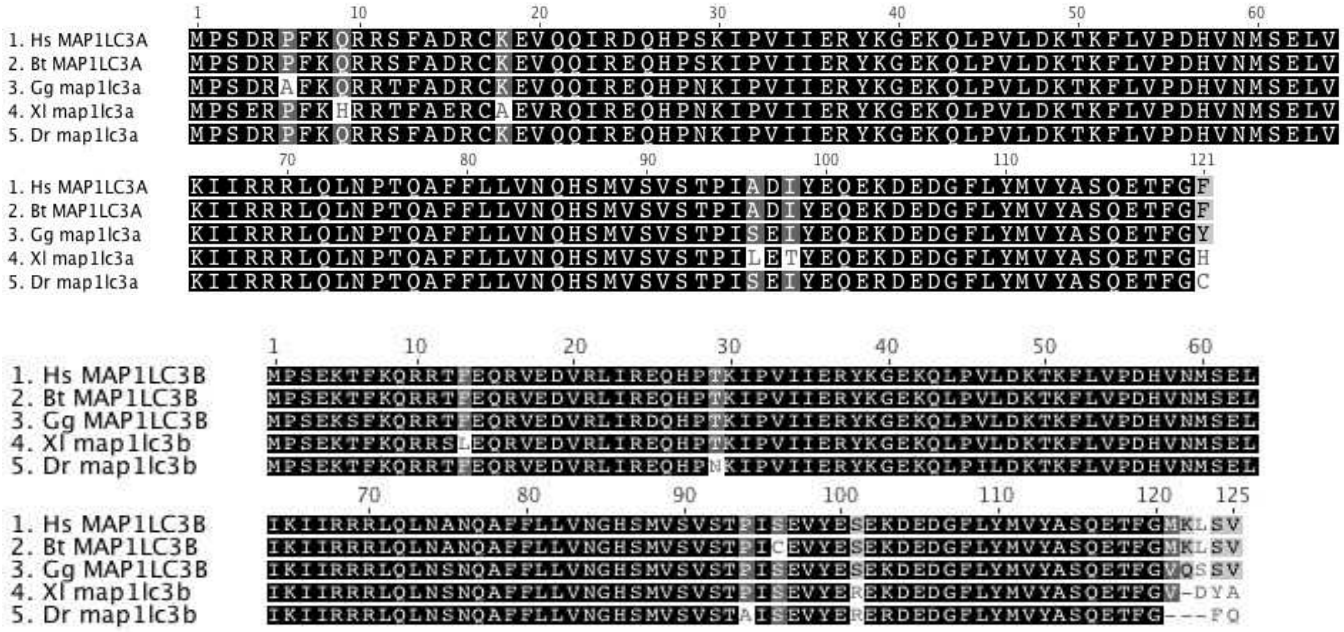

(B)

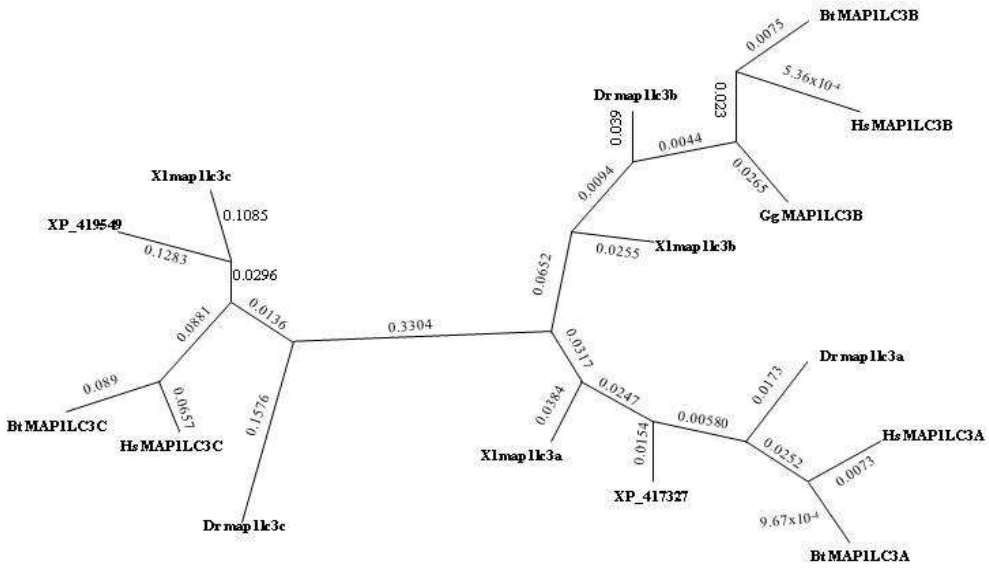
Bt MAP1LC3B
0.0075
5.36x10-4
Hs MAP1LC3B
Dr map1lc3b
0.039
0.023
0.0044
0.0265
Gg MAP1LC3B
0.0094
X1map1lc3b
0.0255
X1map1lc3c
0.1085
XP_419549
0.1283
0.0296
0.0652
0.0881
0.0136
0.3304
0.0317
Dr map1lc3a
0.089
0.0657
0.0247
0.0173
0.00580
Bt MAP1LC3C
Hs MAP1LC3C
0.1576
0.0384
Hs MAP1LC3A
0.0252
0.0154
X1map1lc3a
0.0073
XP_417327
9.67x10-4
Dr map1lc3c
Bt MAP1LC3A

Figure 2 – Schematic showing genes syntenic with the proposed zebrafish orthologue of human *MAP1LC3A* and those syntenic with the human (Hs), mouse (Mm) and bovine (Bt) *MAP1LC3A* genes. The chromosomal positions of these genes are shown on the numbered baselines. Numbers on the baselines indicate gene positions on the chromosomes (M= megabases) (http://www.ensembl.org/Danio_rerio/Info/Index). Arrows indicate the direction of gene transcription. The table shows the orthology relationships between genes in different organisms.

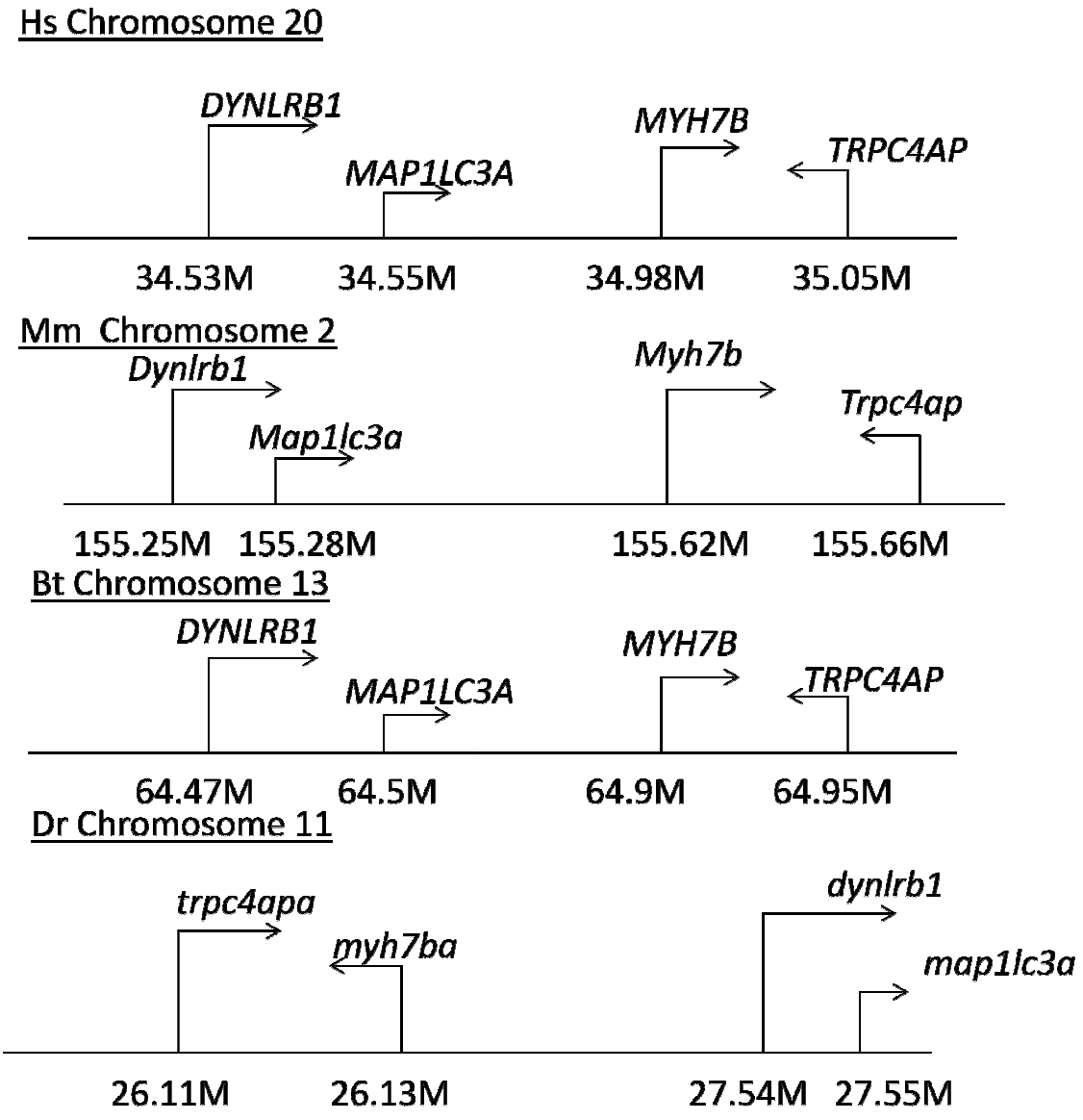

Hs	*Mm*	*Bt*	*Dr*
MAP1LC3A	*Map1lc3a*	*MAP1LC3A*	*map1lc3a*
DYNLRB1	*Dynlrb1*	*DYNLRB1*	*dynlrb1*
TRPC4AP	*Trpc4ap*	*TRPC4AP*	*trpc4apa*
MYH7B	*Myh7b*	*MYH7B*	*myh7ba*

Figure 3 – Schematic showing genes syntenic with the proposed zebrafish orthologue of human *MAP1LC3B* and those syntenic with the human (Hs), mouse (Mm) and bovine (Bt) *MAP1LC3B* genes. The chromosomal positions of these genes are shown on the numbered baselines. Numbers on the baselines indicate gene positions on the chromosomes (M= megabases) (http://www.ensembl.org/Danio_rerio/Info/Index). Arrows indicate the direction of gene transcription. The table shows the orthology relationships between genes in different organisms.

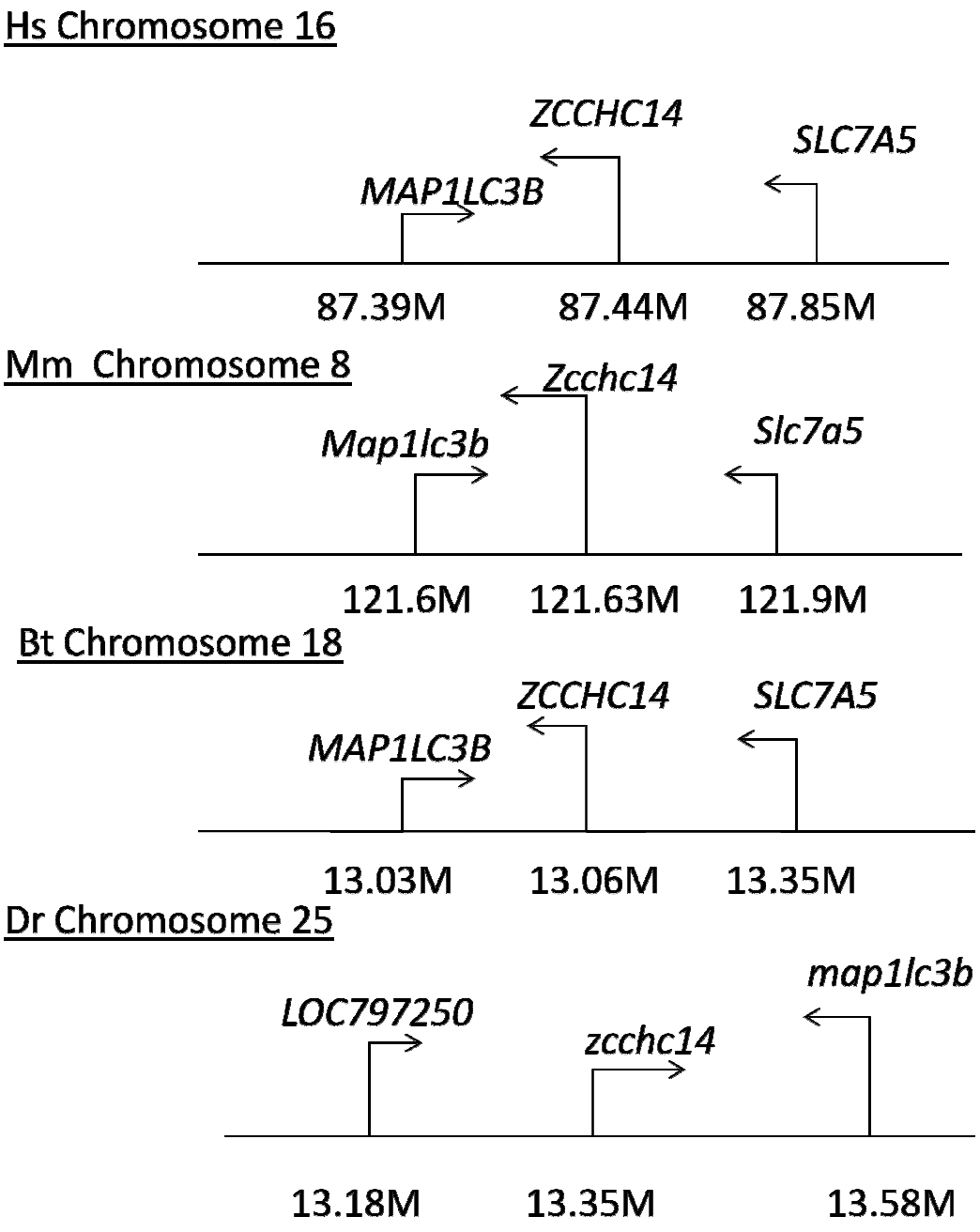

Homo sapiens	*Mus musculus*	*Bos taurus*	*Danio rerio*
MAP1LC3B	*Map1lc3b*	*MAP1LC3B*	*map1lc3b*
ZCCHC14	*Zcchc14*	*ZCCHC14*	*zcchc14*
SLC7A5	*Slc7a5*	*SLC7A5*	*LOC797250*

Figure 4- RT-PCRs detecting *map1lc3a* and *map1lc3b* transcripts at different developmental stages.

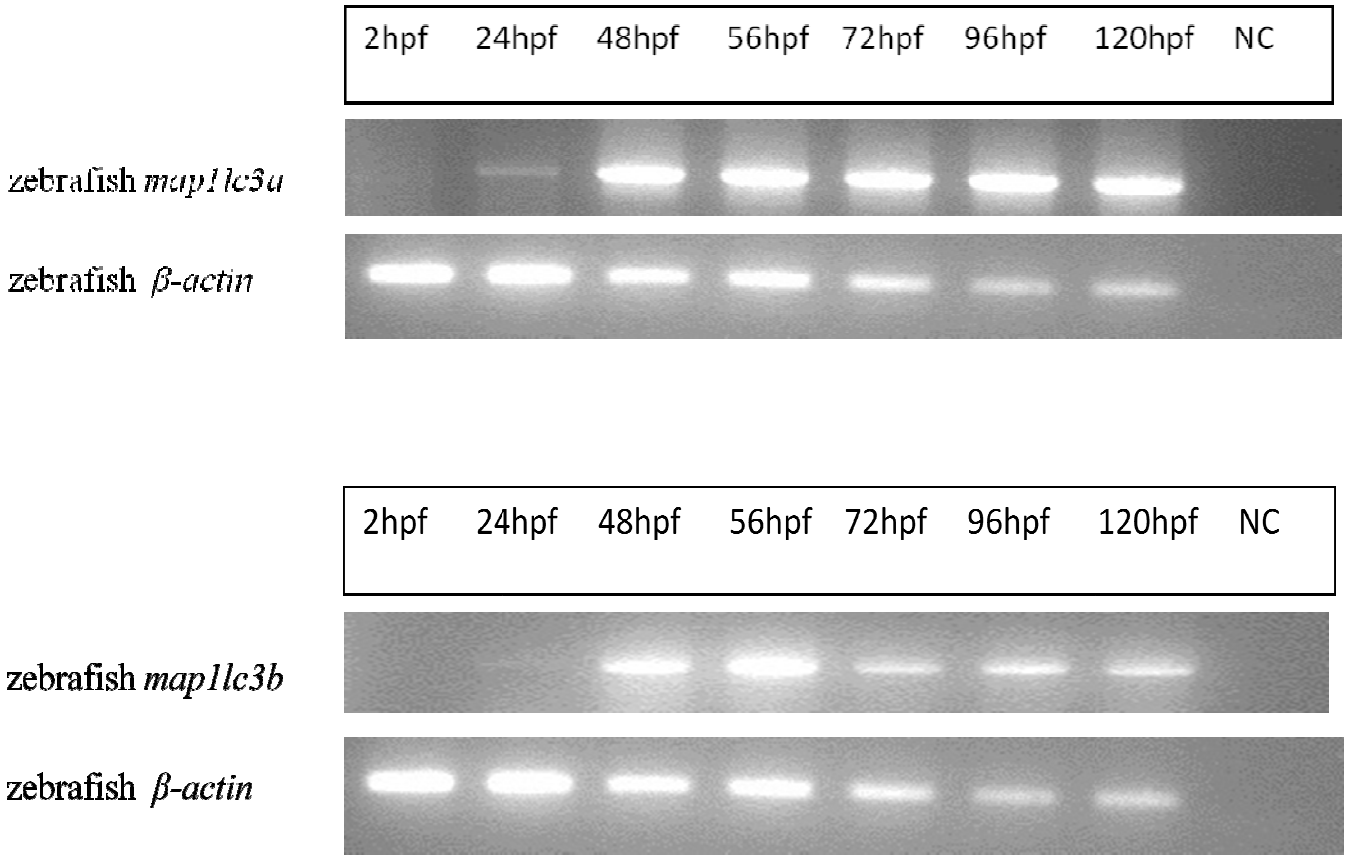

Figure 5 – (A) Relative gene expression level profiles of *map1lc3a* and *map1lc3b* mRNA at different developmental stages determined by qRT-PCR. The expression levels of *map1lc3a* and *map1lc3b* between samples were normalized against *β-actin.* Each experiment was replicated completely three times with triplicate PCRs performed for each replicate. Error bars show standard deviation (S.D).

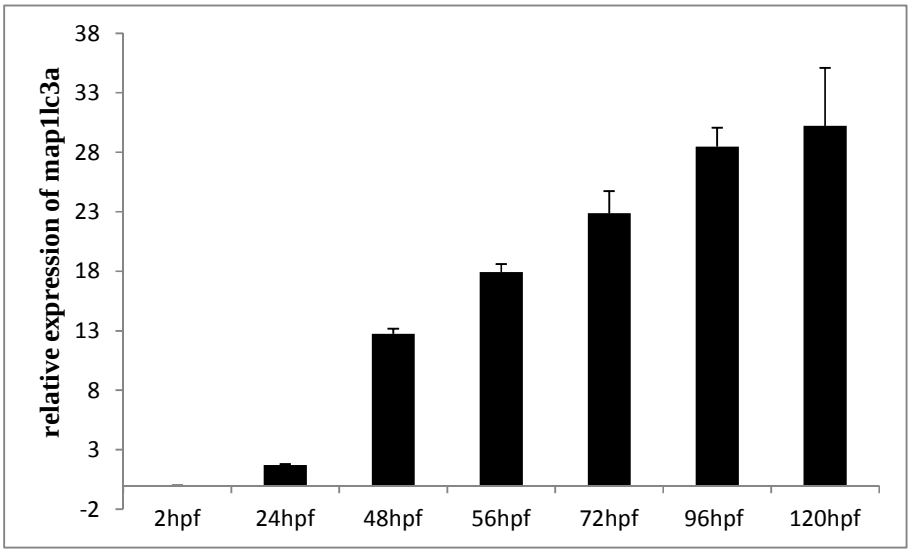

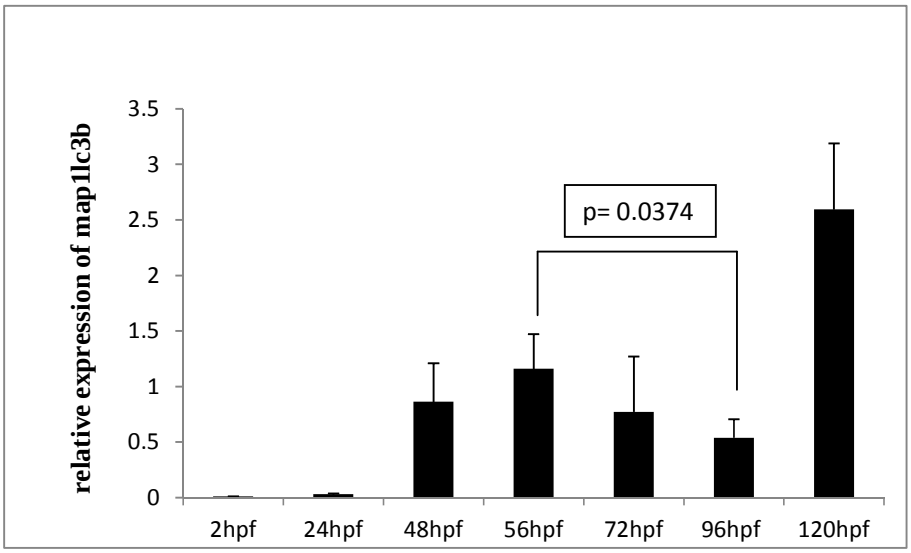

(B) Relative gene expression level profile of *map1lc3a* and *map1lc3b* mRNA at 72h including after exposure to rapamycin and to sodium azide (to mimic hypoxia). The expression levels of *map1lc3a* and *map1lc3b* are normalized against *eef1a1a.* Each experiment was replicated three times and triplicate PCRs were performed for each replicate. Error bars show standard errors of the means.

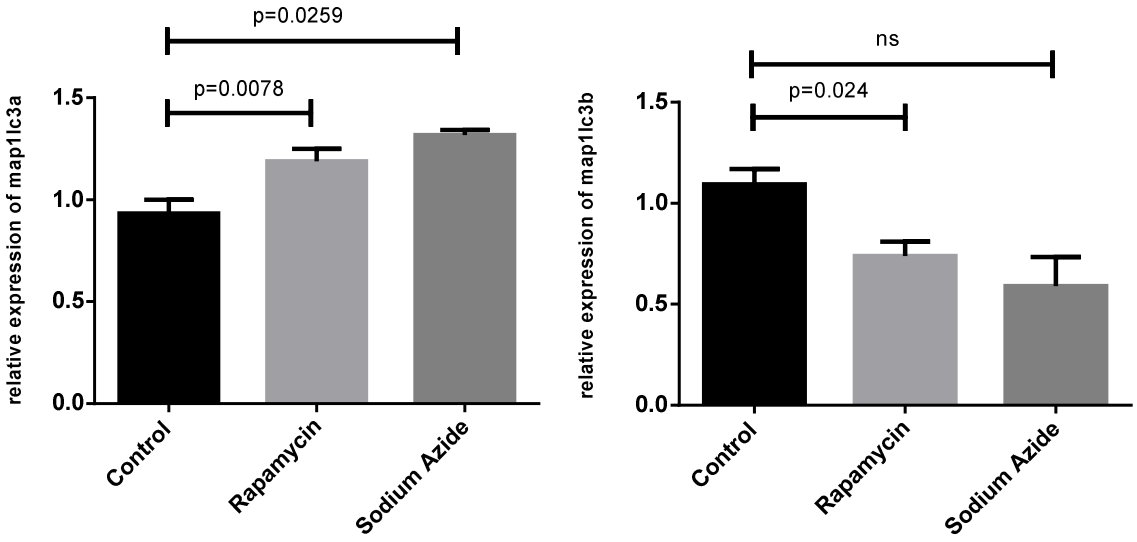

Figure 6 – (A) Use of chloroquine in LC3II/I assays of autophagy in zebrafish larvae. Treatment of embryos with rapamycin or sodium azide was performed as described above. Embryos were deyolked at 72h, lysed and subjected to SDS-PAGE before LC3II and LC3I were detected using anti-LC3 antibody. Anti-tubulin antibody was used as a loading control. (B) The LC3II/LC3I ratio was calculated using Image Lab software. The ratio for the control samples was adjusted to 1.0 and the other ratios were normalised to this. Each analysis was carried out in triplicate. Error bars show standard errors of the means.

Con – Control, Rap - Rapamycin, Chl – Chloroquine, S/A - Sodium Azide.

(A)

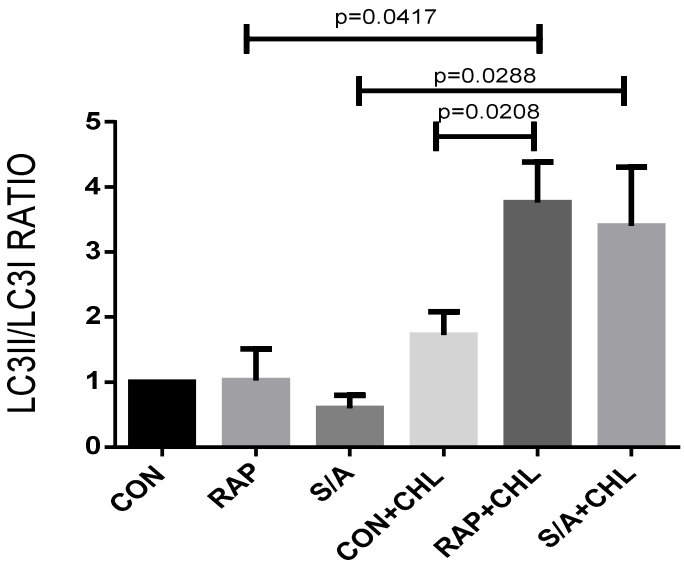

(B)

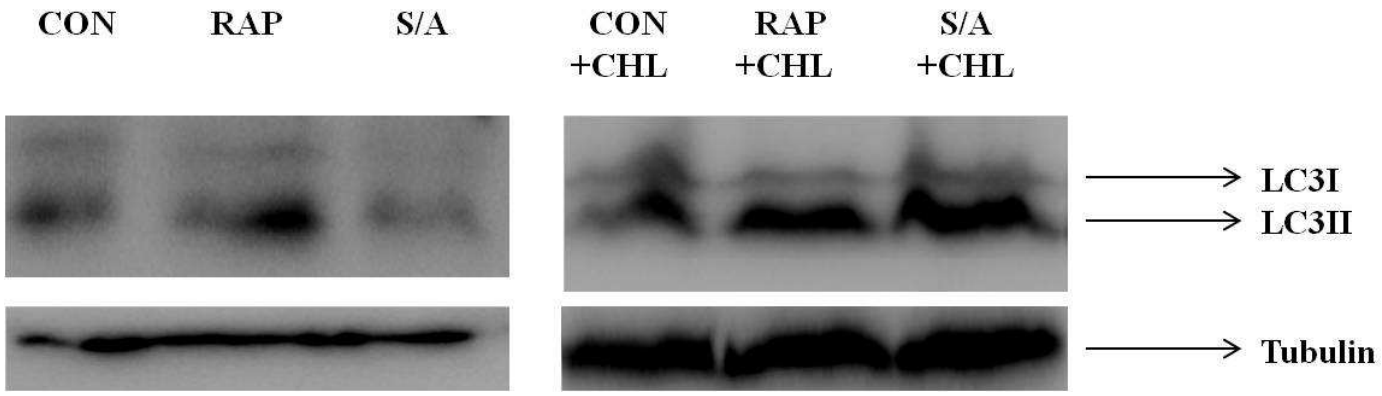

Tables

Table 1 – Protein sequences used in the phylogenetic analysis

Common name	Species name	Sequence	Sequence accession Number
Zebrafish	*Danio rerio*	*map1lc3a*	NP_999904.1
		map1lc3b	NP_955898.1
		map1lc3c	NP_956592.1
Human	*Homo sapiens*	*MAP1LC3A*	NP_115903.1
		MAP1LC3B	NP_073729.1
		MAP1LC3C	NP_001004343.1
Bull	*Bos taurus*	*MAP1LC3A*	NP_001039640.1
		MAP1LC3B	NP_001001169.1
		MAP1LC3C	NP_001094528.1
Chicken	*Gallus gallus*	*MAP1LC3A*	XP_417327.2
		MAP1LC3B	NP_001026632.1
		MAP1LC3C	XP_419549.2
African Clawed Frog	*Xenopus laevis*	*map1lc3a*	NP_001079866.1
		map1lc3b	NP_001089078.1
		map1lc3c	NP_001090411.1

Table 2 – Summary of tBLASTn search results in the analysis of synteny conservation for *map1lc3a*. Highest quality hits are shown in descending order. Probes were translations of full-length open reading frames of the relevant genes.

Probe	Target Organsim	Hits	Quality (E-value)	Probe	Target Organism	Hits	Quality (E-value)
Human DYNLRB1	Zebrafish	NM_201188.1	$5e^{-53}$	Zebrafish dynlrb1	Human	NM_014183.2	$1e^{-52}$
Human TRPC4AP	Zebrafish	NM_131569.2	0.0	Zebrafish Trpc4apa	Human	NM_015638.2	0.0
Human MYH7B	Zebrafish	XM_001335708.3	0.0	Zebrafish Myh7b	Human	NM_020884.3	0.0

Table 3 – Summary of tBLASTn search results in the analysis of synteny conservation for *map1lc3b*. Highest quality hits are shown in descending order. Probes were translations of full-length open reading frames of the relevant genes.

Probe	Target Organsim	Hits	Quality (E-value)	Probe	Target Organism	Hits	Quality (E-value)
Human SLC7A5	Zebrafish	NM_001128358.1	0.0	Zebrafish	Human	NM_003486.5	0.0
Human ZCCHC14	Zebrafish	XM_001336490.4	$9e^{-89}$	Zebrafish	Human	NM_015144.2	$9e^{-96}$